Robust Chaos in Systems of Circular Geometry

V. M. Doroshenko[1, 2], **V. P. Kruglov**[3], **and M. V. Pozdnyakov**[2]

[1]Saratov State University, Russia
[2]Saratov State Medical University, Russia
[3]Saratov Branch of Kotelnikovs Institute of Radio-Engineering and Electronics of RAS, Russia

Abstract— We propose two models of systems that manifest robust chaotic regimes associated with uniformly hyperbolic attractors. The model schemes are rings of oscillators and nonlinear elements arranged in such way that signals undergo special transformation during full rotation along the rings. The models are governed by systems of ordinary differential equations. These equations were studied numerically. We discuss the results of numerical simulation that confirm our suggestion of robust hyperbolic chaos in proposed models.

1. INTRODUCTION

Uniformly hyperbolic attractors have strong chaotic properties [1–6]. Unlike most strange attractors the hyperbolic ones are robust [1–6]. That means the structure of attractor preserves under relatively small perturbations of governing equations or under small changes of parameters. Smale–Williams solenoid is a well-known example of uniformly hyperbolic attractor [1]. It can arise in phase space of dimension 3 (or higher) under discrete-time mapping which one can describe geometrically as stretching along some angular variable in integer number of times and strong contraction in other directions of some toroid with folding of the image inside preimage domain.

Once it was believed that uniformly hyperbolic attractors describe chaotic behavior in many cases. Now hyperbolic attractors are seem to be rare and most known chaotic attractors are non-hyperbolic. Only recently some physically realizable examples were introduced [6–8].

We discuss some systems of circular geometry introduced by us. These systems demonstrate robust chaotic regimes associated with uniformly hyperbolic attractors of Smale–Williams type in Poincaré cross-section. The operation of proposed systems is based on angular variable transformation of special kind [6–8]. The systems are designed so that some angular variable (e.g., phase of oscillations) undergoes Bernoulli map on each average time interval, while the phase space strongly contracts in other directions. After many times, asymptotically, it leads to Smale–Williams solenoid arise.

2. CIRCULAR NONAUTONOMOUS ROBUST CHAOS GENERATOR OF TWO LINEAR OSCILLATORS AND TWO NONLINEAR ELEMENTS

The first model is a ring of two linear oscillators and two nonlinear elements (Fig. 1). x and y are the output signals of oscillators. The natural frequency of the second oscillator is twice as large the frequency of the first oscillator ω_0. The output $f(x^2)$ of the first nonlinear element is quadratic at low amplitudes of input signal x and saturates at high amplitudes. The second nonlinear element multiplies the signal from the second oscillator y and an external signal $g(t)$.

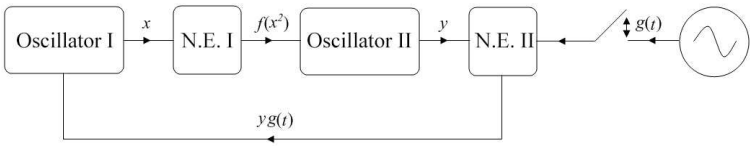

Figure 1: A block scheme of the system.

The function $f(x^2) = \frac{x^2}{1+x^2}$ describes the transformation of a signal on the first nonlinear element. The function $g(x) = \begin{cases} a^2 \sin^2(\frac{\pi t}{\tau}) \sin(\omega_0 t), & \text{if } 0 \leqslant t \leqslant \tau; \\ 0, & \text{if } \tau < t \leqslant T \end{cases}$ describes the external signal.

Governing equations in dimensionless variables appear as follows:

$$\begin{aligned} \dot{x} &= -\omega_0 u - \gamma x + \gamma g(t) y, \\ \dot{u} &= \omega_0 x, \\ \dot{y} &= -2\omega_0 v - \gamma y + \gamma \frac{x^2}{1+x^2}, \\ \dot{v} &= 2\omega_0 y, \end{aligned} \tag{1}$$

Excitation transfer between subsystems is resonant. Resonant excitation allows implementing necessary transformation of phase in wide range of parameters.

Let's discuss operation of the system. Suppose first that the external signal is turned off and the first oscillator performs decaying harmonic oscillations at the frequency ω_0 with the phase ϕ. When the signal from the first oscillator passes through the first non-linear element, the second harmonics appear with double phase and frequency. The second harmonic is in resonance with the natural frequency of the second oscillator and excites oscillations in it with double phase. If the auxiliary signal is turned on it mixes with the signal from the second oscillator. As a result, the signal component appears with a phase 2ϕ and a frequency close to ω_0. This component excites the first oscillator and transmits its phase. Thus through each period of the external action phase of the oscillations is doubled, and its dynamics is approximately described by the Bernoulli map: $\phi_{n+1} = 2\phi_n + \text{const} \pmod{2\pi}$, where n is number of a period, and the constant takes into account phase additive under the transmission of signal from one oscillator to the other (it can be eliminated by shifting the reference point).

Since the scheme is described by a non-autonomous system of the fourth order differential equations, the phase space of the system (including time) is five-dimensional. To study the attractor of the system it is convenient to go to the Poincaré map over the period of external action with four-dimensional space of instantaneous states. One can take a hyperplane $t_n = nT$ in the extended phase space as the intersecting surface, where T is the period of external action, n is the number of the period.

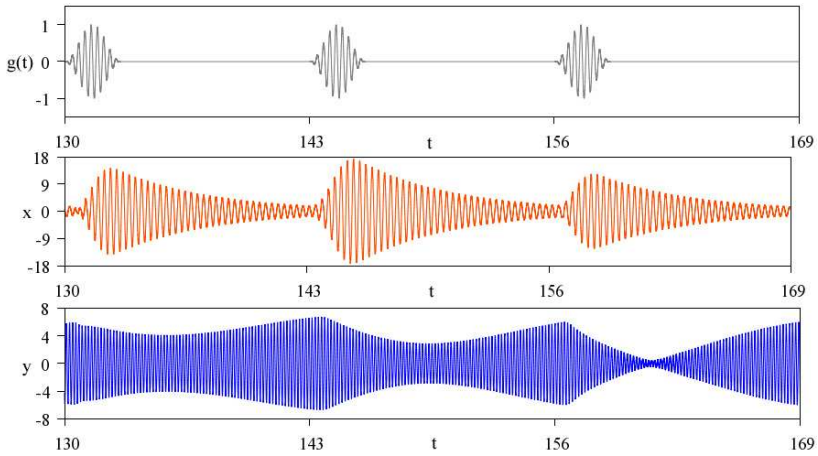

Figure 2: Time dependences of the dynamical variables x and y and time dependence of function $g(t)$ for the parameter values $\omega_0 = 6\pi,\ \tau = 3,\ T = 13,\ a = 24,\ \gamma = 0.4$

The system of Equation (1) was solved numerically by the Runge–Kutta fourth order method in increments of 0.001. Fig. 2 shows the time dependences of the dynamical variables x and y and time dependence of function $g(t)$ during three periods of external action for the parameter values $\omega_0 = 6\pi,\ \tau = 3,\ T = 13,\ a = 24,\ \gamma = 0.4$. Chaos in the system manifests itself in the irregular variation of the phases and peak amplitudes of the oscillators on consecutive periods of the external signal.

Figure 3 shows the attractor of the Poincaré map for the period of the external action in the projection onto the plane (x, u) and its enlarged detail. The portrait is visually similar to the attractor of the Smale–Williams; this suggests that the system has a uniformly hyperbolic attractor. Fractal structure of the attractor is clearly visible.

Figure 4 shows an iterative diagram of the Poincaré map for the phase of the second oscillator for the parameter values $\omega_0 = 6\pi,\ \tau = 3,\ T = 13,\ a = 24,\ \gamma = 0.4$. Phase belongs to the interval

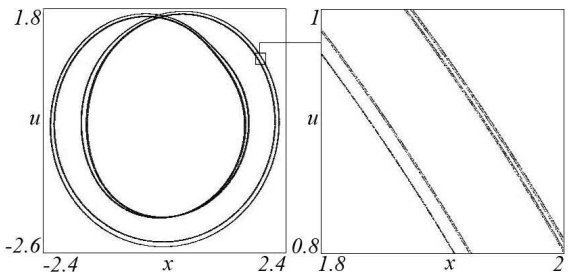

Figure 3: The attractor of the Poincaré map for the period of the external action in the projection onto the plane (x, u) and its enlarged detail for the parameter values $\omega_0 = 6\pi,\ \tau = 3,\ T = 13,\ a = 24,\ \gamma = 0.4$.

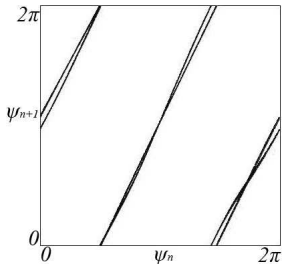

Figure 4: Iterative diagram of the Poincaré map for the phase of the second oscillator for the parameter values $\omega_0 = 6\pi,\ \tau = 3,\ T = 13,\ a = 24,\ \gamma = 0.4$.

from 0 to 2π and is defined by the expression $\psi = \arg(y + iv)$. As we can see from the diagram, the phase dynamics is described approximately by Bernoulli map: for the full passage of point from 0 to 2π its image passes this interval twice.

Calculation of the Lyapunov exponents allows identifying the dynamic regime of the system. For attractor in the Poincaré cross-section Lyapunov exponents were computed by a known algorithm [9, 10]. For parameters $\omega_0 = 6\pi,\ \tau = 3,\ T = 13,\ a = 24,\ \gamma = 0.4$ the full spectrum of Lyapunov exponents was obtained

$$\Lambda_1 = 0.684 \pm 0.004, \quad \Lambda_2 = -2.11 \pm 0.02, \quad \Lambda_3 = -3.67 \pm 0.04, \quad \Lambda_4 = -5.28 \pm 0.02.$$

The largest Lyapunov exponent is positive, which is a quantitative confirmation of the presence of chaos. It is close to the value of $\ln 2$ or the Lyapunov exponent of Bernoulli map, which approximately describes the dynamics of the phase oscillations in the system. Other exponents are negative. Thus, the element of volume in the phase space of the Poincaré map expands in one direction and contracts of the other three during the one iteration. This corresponds to the

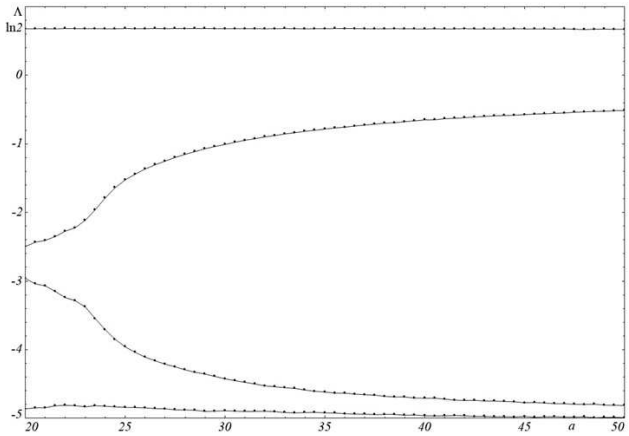

Figure 5: The dependences of the Lyapunov exponents for the attractor of the Poincaré map from the amplification coefficient a at fixed values of other parameters ($\omega_0 = 6\pi,\ \tau = 3,\ T = 13, \gamma = 0.4$).

construction of a hyperbolic attractor of the Smale-Williams type (given that there is stretching of the angular variable), but in four-dimensional phase space.

Figure 5 shows the dependences of the Lyapunov exponents for the attractor of the Poincaré map from the amplification coefficient a at fixed values of other parameters ($\omega_0 = 6\pi,\ \tau = 3,\ T = 13, \gamma = 0.4$). The oldest exponent is positive and the others are negative throughout the interval of variation of parameter a. The largest exponent depends smoothly on the parameter; sharp dips to the negative values are missing which is typical for robust regimes. The value of the largest exponent remains close to $\ln 2$ in a wide range of the parameter.

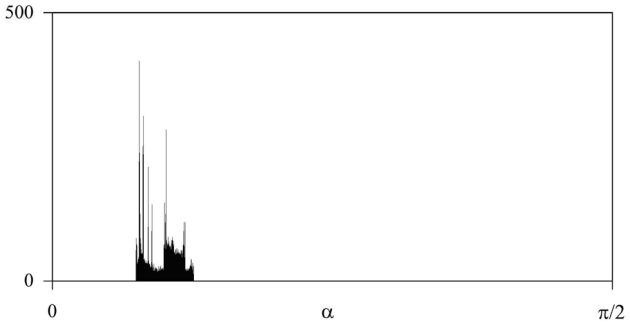

Figure 6: The distribution of angles between stable and unstable subspaces of the attractor for the parameter values $\omega_0 = 6\pi,\ \tau = 3,\ T = 13,\ a = 24,\ \gamma = 0.4$.

Numerical test to confirm hyperbolicity of attractor was performed [11–14]. Nonexistence of zero angles between stable and unstable manifolds of trajectories is a required property of uniformly hyperbolic attractor. The statistics of angles was accumulated for a number of sufficiently long typical trajectories on attractor. Fig. 6 shows the distribution of angles between stable and unstable subspaces. Intersections with zero and close to zero angles are absent. This confirms the suggestion of uniformly hyperbolic attractor.

3. CIRCULAR NONAUTONOMOUS ROBUST CHAOS GENERATOR BASED ON "OSCILLATION DEATH"

The operation of the second model is based on "oscillation death". It is composed of van der Pol oscillator and linear oscillator. x and y are the output signals of oscillators. The natural frequency of the linear oscillator is twice as large the frequency of the self-oscillator ω_0. Signals between the oscillators circulate through nonlinear elements described by functions εx^2 and $2\varepsilon xy$. The oscillations of the self-oscillator are periodically killed by $KH(\sin(2\pi t/T))(\dot{y} - \dot{x})$, where $H(\xi) = \begin{cases} 0, & \text{if } \xi < 0, \\ 1, & \text{if } \xi \geqslant 0, \end{cases}$ is Heaviside function.

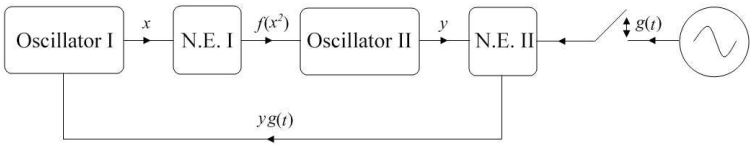

Figure 7: A block scheme of the system.

Governing equations in dimensionless variables are:

$$\begin{aligned} &\dot{x} = u, \\ &\dot{u} = (\mu - x^2)u - \omega_0^2 x - 2\varepsilon xy + KH(\sin(2\pi t/T))(v - u), \\ &\dot{y} = v, \\ &\dot{v} = -\alpha v - 4\omega_0^2 y - \varepsilon x^2, \end{aligned} \tag{2}$$

Let's discuss operation of the system. Suppose first that the $H(\sin(2\pi t/T)) = 0$ and the van der Pol oscillator performs self-oscillations at the frequency ω_0 with the phase ϕ. The signal εx^2 slowly excites oscillations in the linear oscillator with frequency $2\omega_0$ and phase 2ϕ. When $H(\sin(2\pi t/T))$

becomes equal to one the term $(\dot{y}-\dot{x})$ drives the self-oscillator away from limit cycle-like behaviour to equilibria-like state. When $H(\sin(2\pi t/T))$ becomes equal to zero again the self-oscillator starts to oscillate, synchronizes with signal $2\varepsilon xy$ and gets phase 2ϕ. Through each period of the modulation the phase of the oscillations is doubled, and its dynamics is approximately described by the Bernoulli map.

Equations (2) were solved numerically by the Runge-Kutta fourth order method in increments of 0.001. Fig. 8 demonstrates the time realizations of the dynamical variables x and y in the steady state and time dependence of function $H(\sin(2\pi t/T))$ during three periods of external action for the parameter values $\omega_0 = 2\pi,\ \mu = 1.5,\ T = 20,\ \alpha = 0.4,\ \varepsilon = 0.5,\ K = 5$. Chaos in the system appears in irregular variation of the phases of the oscillators on consecutive periods of modulation.

We obtained numerically the Poincaré map over the period of modulation with hyperplanes $t_n = nT$ as the intersecting surfaces, where T — period of external action, n — number of the period.

Figures 9 and 10 show the attractor of the Poincaré map for the period of the modulation and iterative diagrams for the phases. The portraits are visually similar to the attractor of the Smale-Williams. Fractal structure of the attractor on Fig. 10 is clearly visible. As one can see from the diagrams, the phase evolution is described approximately by expanding map of the circle.

For attractor in the Poincaré cross-section Lyapunov exponents were computed. For parameters $\omega_0 = 2\pi,\ \mu = 1.5,\ T = 20,\ \alpha = 0.4,\ \varepsilon = 0.5,\ K = 5$ the full spectrum of Lyapunov exponents was obtained

$$\Lambda_1 = 0.626 \pm 0.009, \quad \Lambda_2 = -1.266 \pm 0.004, \quad \Lambda_3 = -17.74 \pm 0.02, \quad \Lambda_4 = -19.93 \pm 0.03.$$

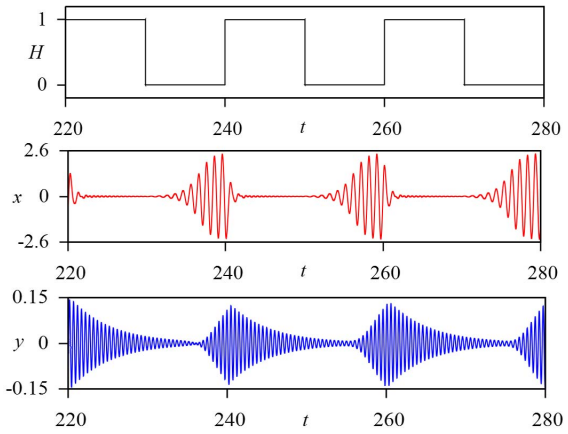

Figure 8: Time dependences of the dynamical variables x and y and time dependence of function $H(\sin(2\pi t/T))$ for the parameter values $\omega_0 = 2\pi,\ \mu = 1.5,\ T = 20,\ \alpha = 0.4,\ \varepsilon = 0.5,\ K = 5$.

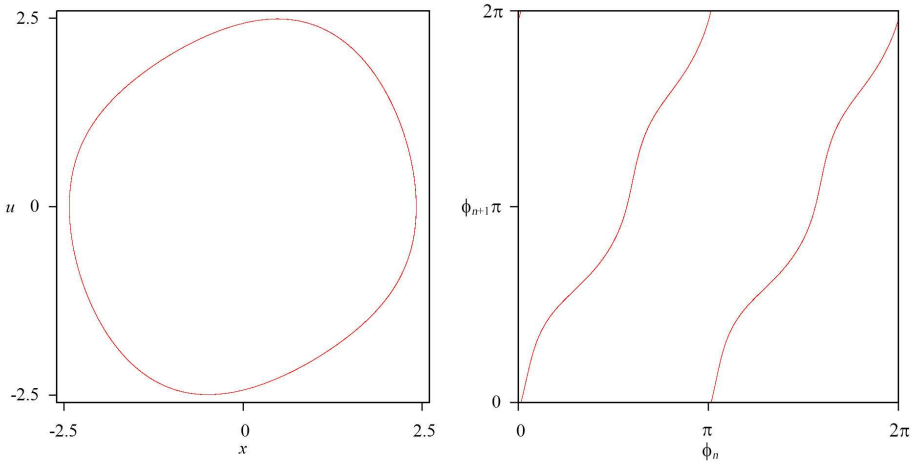

Figure 9: The attractor of the Poincaré map for the period of the modulation in the projection onto the plane (x, u) for the parameter values $\omega_0 = 2\pi,\ \mu = 1.5,\ T = 20,\ \alpha = 0.4,\ \varepsilon = 0.5,\ K = 5$. Iterative diagram of the Poincaré map for the phase $\phi = \arg(x + iu)$.

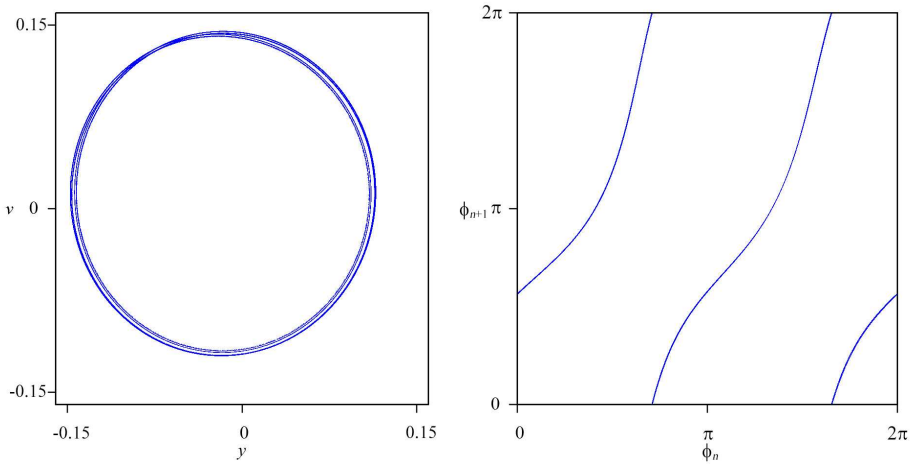

Figure 10: The attractor of the Poincaré map for the period of the modulation in the projection onto the plane (y, v) for the parameter values $\omega_0 = 2\pi,\ \mu = 1.5,\ T = 20,\ \alpha = 0.4,\ \varepsilon = 0.5,\ K = 5$. Iterative diagram of the Poincaré map for the phase $\phi = \arg(y + iv)$.

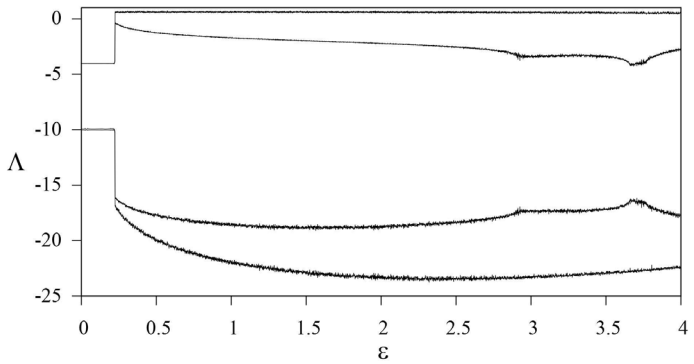

Figure 11: The dependences of the Lyapunov exponents for the attractor of the Poincaré map from ε at fixed values of other parameters $\omega_0 = 2\pi,\ \mu = 1.5,\ T = 20,\ \alpha = 0.4,\ K = 5$.

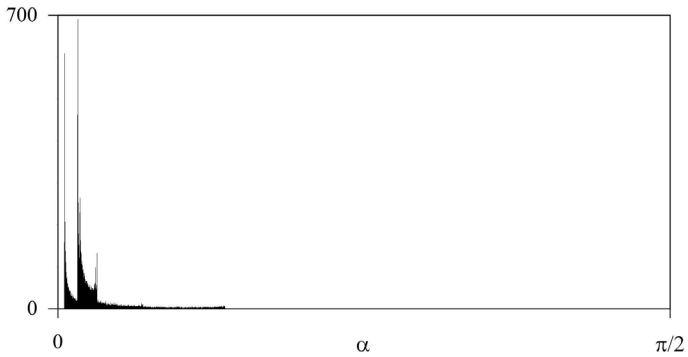

Figure 12: The distribution of angles between stable and unstable subspaces of the attractor for the parameter values $\omega_0 = 2\pi,\ \mu = 1.5,\ T = 20,\ \alpha = 0.4,\ \varepsilon = 0.5,\ K = 5$.

The largest Lyapunov exponent is positive and close to the value of Lyapunov exponent of Bernoulli map ($\ln 2$). Other exponents are negative. This corresponds to the construction of a hyperbolic attractor of the Smale–Williams type in four-dimensional phase space. Fig. 11 shows the dependence of the Lyapunov exponents for the attractor of the Poincaré map from ε at fixed values of other parameters. The oldest exponent is positive on wide range of variation of parameter ε and the others are negative throughout this interval. The largest exponent depends smoothly on the parameter; sharp dips to the negative values are absent which indicates robust regime. The value of the largest exponent remains close to $\ln 2$.

Numerical test to confirm hyperbolicity of attractor was performed. The statistics of angles

between stable and unstable subspaces of attractor was accumulated for a number of sufficiently long typical trajectories on attractor. Fig. 12 shows the distribution of angles between stable and unstable subspaces. Intersections with zero and close to zero angles were not found. This allows us to assume that attractor is uniformly hyperbolic.

4. CONCLUSION

We suggest two models of robust chaos generators. The models were studied numerically. Our results (portraits of attractors, iteration diagrams for phases, Lyapunov exponents) let us assume that proposed systems demonstrate robust chaotic regimes associated with Smale–Williams solenoid. We also performed numerical tests in which we checked nonexistence of zero angles between stable and unstable manifolds of trajectories, which is a required property of uniformly hyperbolic attractor. The considered systems are valuable due to their robustness and may be implemented in electronics.

ACKNOWLEDGMENT

This work was supported by RFBR grant No 16-32-00449. The work of V.P.K. was partially supported by RFBR grant No. 16-02-00135.

REFERENCES

1. Smale, S., "Differentiable dynamical systems," *Bull. Amer. Math. Soc.*, Vol. 73, No. 6, 747–817, 1967.
2. Williams, R. F., "Expanding Attractors," *Publ. Math. Inst. Hautes Etudes Sci.*, Vol. 43, No. 10, 169–203, 1974.
3. Katok, A. and B. Hasselblatt, "Introduction to the modern theory of dynamical systems," *Encyclopedia Math. Appl.*, Vol. 54, Cambridge University Press, Cambridge, 1995.
4. Anosov, D. V., "Dynamical systems 9: Dynamical systems with hyperbolic behaviour," *Encyclopaedia Math. Sci.*, Vol. 66, Springer, Berlin, 1995.
5. Afraimovich, V. and S.-B. Hsu, "Lectures on chaotic dynamical systems," *AMS/IP Stud. Adv. Math.*, Vol. 28, R.I.: AMS, Providence, 2003.
6. Kuznetsov, S. P., *Hyperbolic Chaos: A Physicists View*, Springer, Berlin, 2012.
7. Kuznetsov, S. P., "Example of a physical system with a hyperbolic attractor of the Smale-Williams type," *Phys. Rev. Lett.*, Vol. 95, No. 14, 144101, 2005.
8. Kuznetsov, S. P. and A. Pikovsky, "Autonomous coupled oscillators with hyperbolic strange attractors," *Phys. D*, Vol. 232, No. 2, 87–102, 2007.
9. Benettin, G., L. Galgani, A. Giorgilli, and J.-M. Strelcyn, "Lyapunov characteristic exponents for smooth dynamical systems and for hamiltonian systems: A method for computing all of them. P.1: Theory; P.2: Numerical Application," *Meccanica*, Vol. 15, 9–30, 1980.
10. Shimada, I. and T. Nagashima, "A numerical approach to ergodic problem of dissipative dynamical systems," *Prog. Theor. Phys.*, Vol. 61, 1605–1616, 1979.
11. Lai, Y.-C., C. Grebogi, J. A. Yorke, and I. Kan, "How often are chaotic saddles nonhyperbolic?," *Nonlinearity*, Vol. 6, 779–798, 1993.
12. Anishchenko, V. S., A. S. Kopeikin, J. Kurths, T. E. Vadivasova, and G. I. Strelkova, "Studying hyperbolicity in chaotic systems?," *Physics Letters A.*, Vol. 270, 301–307, 2000.
13. Kuptsov, P. V., "Fast numerical test of hyperbolic chaos," *Phys. Rev. E.*, Vol. 85, No. 1, 015203, 2012.
14. Kuznetsov, S. P. and V. P. Kruglov, "Verification of hyperbolicity for attractors of some mechanical systems with chaotic dynamics," *Regular and Chaotic Dynamics*, Vol. 21, No. 2, 160–174, 2016.